$\pi-\pi$ Interactions in Organometallic Systems. Crystal Structures and Spectroscopic Properties of Luminescent Mono-, Bi-, and Trinuclear Trans-cyclometalated Platinum(II) Complexes Derived from 2,6-Diphenylpyridine

Wei Lu, Michael C. W. Chan, Kung-Kai Cheung, and Chi-Ming Che*

Department of Chemistry, The University of Hong Kong, Pokfulam Road, Hong Kong SAR, China

Received November 20, 2000

A series of mono- and multinuclear dicyclometalated platinum(II) complexes, namely, [Pt(C^N^C)L[1]] [HC^N^CH = 2,6-diphenylpyridine; L^1 = 4-*tert*-butylpyridine (**1**), 1-methyl-4,4′-bipyridinium (MQ^+) hexafluorophosphate (**2**(PF_6)), 2,6-dimethylphenylisocyanide (**4**), tricyclohexylphosphine (**5**), triphenylphosphine (**7**)], [Pt_2(C^N^C)$_2$(μ-L^2)] [L^2 = pyrazine (pyr; **3**), bis(dicyclohexylphosphino)methane (dcpm; **6**), bis(diphenylphosphino)methane (dppm; **8**)], and [Pt_3(C^N^C)$_3$(μ_3-dpmp)] [dpmp = bis(diphenylphosphinomethyl)phenylphosphine (**9**)], were synthesized from [Pt(C^N^C)dmso] (dmso = dimethyl sulfoxide). The X-ray crystal structures of **1**, **3**·$CHCl_3$, **4**, **6**·$CHCl_3$·CH_3OH·$4H_2O$, **7**, **8** (yellow form), and **8**·$CHCl_3$ (orange form) have been determined. For complex **1**, the Pt(C^N^C) units are oriented into pairs in a head-to-tail fashion with an interplanar separation of 3.40 Å. For complex **4**, dimeric $\pi-\pi$ overlap between Pt(C^N^C) and phenyl moieties in a head-to-tail manner is observed, with interplanar stacking at 3.39 Å. There are two crystal forms for complex **8**. Only one intramolecular Pt(C^N^C)−phenyl $\pi-\pi$ interaction (separation 3.381 Å) is apparent in the yellow form. For the orange form (**8**·$CHCl_3$), there are two intramolecular Pt(C^N^C)−phenyl $\pi-\pi$ contacts (separations 3.115 and 3.287 Å). For **3**·$CHCl_3$, the dihedral angles between the pyrazine and the two Pt(C^N^C) planes are 124.0° and 130.5°, which allows the possibility for partial orbital interaction between the (5d)Pt and pπ*(pyrazine) orbitals. Complexes **1** and **4**−**9** display vibronically structured emission (λ_{max} of most intense band = 508−526 nm) in 77 K methanol/ethanol (1:5, v/v) glass, which are assigned to ^{3}IL excited states. For **1**, **4**−**6**, **8**, and **9**, the 77 K structureless emission at λ_{max} 596−636 nm in methanol/ethanol glasses is assigned as $\pi\pi$* excimeric in nature. These excimeric emissions are concentration-dependent for **1** and **4**−**6** and concentration-independent for **8** and **9**. The 298 K solid emission spectra of **1**, **4**−**6**, **8**, and **9** are characterized by a broad, unstructured band at λ_{max} 566−633 nm, which red-shift in energy upon cooling to 77 K. These bands are comparable in energy to the 77 K glassy emissions and are similarly assigned. Complexes **2** and **3** show an intense absorption at λ_{max} 410 (shoulder) and 456 nm, which are ascribed to the MLCT (5d)Pt → π*(1-methyl-4,4′-bipyridinium/pyrazine) transition, respectively. Likewise, the solid-state emissions of **2** and **3** at λ_{max} 686 and 658 nm, respectively, are assigned as MLCT. The vapochromism of complex **8** has been investigated.

Introduction

Noncovalent contacts are essential for molecular recognition, and the significance of attractive interactions between aromatic π-systems in supramolecular chemistry and life sciences has been established.[1−3] Indeed, $\pi-\pi$ interactions have been recognized as a solid-state and dynamic design motif and incorporated into many topical areas of research such as crystal engineering, self-assembly, and molecular machines and electronics.[4−9] Previous investigations on π-stacking interactions in transition metal complexes have often focused on nucleobases and related ligands.[10] The

* Author to whom correspondence should be sent. Fax: (852) 2857 1586. E-mail: cmche@hku.hk.

(1) Lehn, J. M. *Angew. Chem., Int. Ed. Engl.* **1990**, *29*, 1304.
(2) Saenger, W. *Principles of Nucleic Acid Structure*; Springer-Verlag: New York, 1984.
(3) Hunter, C. A.; Sanders, J. K. M. *J. Am. Chem. Soc.* **1990**, *112*, 5525.
(4) Desiraju, G. R. *Angew. Chem., Int. Ed. Engl.* **1995**, *34*, 2311.
(5) Coates, G. W.; Dunn, A. R.; Henling, L. M.; Dougherty, D. A.; Grubbs, R. H. *Angew. Chem., Int. Ed. Engl.* **1997**, *36*, 248.
(6) Hirsch, K. A.; Wilson, S. R.; Moore, J. S. *Chem. Eur. J.* **1997**, *3*, 765.
(7) Cochran, J. E.; Parrott, T. J.; Whitlock, B. J.; Whitlock, H. W. *J. Am. Chem. Soc.* **1992**, *114*, 2269.
(8) Ashton, P. R.; Huff, J.; Menzer, S.; Parsons, I. W.; Preece, J. A.; Stoddart, J. F.; Tolley, M. S.; White, A. J. P.; Williams, D. J. *Chem. Eur. J.* **1996**, *2*, 31.
(9) Collier, C. P.; Wong, E. W.; Belohradský, M.; Raymo, F. M.; Stoddart, J. F.; Kuekes, P. J.; Williams, R. S.; Heath, J. R. *Science* **1999**, *285*, 391.

10.1021/om0009839 CCC: $20.00
Publication on Web 05/11/2001

discipline of organometallic crystal engineering is still in its infancy, particularly with respect to the design and employment of $\pi-\pi$ stacking attractions.[11] Nevertheless, structural examples of $\pi-\pi$ interactions between cyclometalated diimine and analogous polypyridyl ligands have been reported by our group[12−20] and other researchers.[21−25] For example, we recently described a class of mono- and binuclear luminescent trans-cyclometalated gold(III) complexes derived from 2,6-diphenylpyridine, and perturbations in emissive behavior were ascribed as consequences of subtly different intramolecular $\pi-\pi$ contacts.[17] In our pursuit to develop luminescent sensory materials, we have been studying the correlation between $\pi-\pi$ interactions and photoluminescence in platinum(II) complexes. A deeper appreciation of these photophysical manifestations arising from noncovalent contacts may ultimately lead to new developments in functional photonic materials.

Coordinatively unsaturated platinum(II) luminophores[26] and their application as molecular sensors[27] have generated immense interest in recent years. Many investigations have shown that the color and emissive properties of crystalline Pt(II) diimine salts are highly dependent upon the chosen anion and solvent(s) for the precipitation/recrystallization,[23,24,26c,28,29] and differences in the extent of $\pi-\pi$ and/or Pt−Pt interactions are usually cited to rationalize these phenomena. Following work on the [Au(C^N^C)L]$^+$ system (HC^N^CH = 2,6-diphenylpyridine),[17] we turned our attention toward the isoelectronic Pt(II) congeners as part of a program to develop neutral luminescent organoplatinum(II) materials that are stable with respect to sublimation for organic light-emitting device (OLED) applications. Complexes of the type [Pt(C^N^C)L] (L = Et_2S, pyridine, pyrazine) were first reported by von Zelewsky and co-workers. Their emissions in 77 K alcoholic glasses were assigned to an MLCT (L = C^N^C) excited state with some intraligand (IL) contribution,[30] but no details of crystal structures and photophysical properties were reported. Recent work by Rourke and co-workers offered a readily accessible synthetic route to the [Pt(C^N^C)] moiety in high yield.[31] We now present the preparation and structural and photophysical characterization of mono-, bi-, and trinuclear trans-cyclometalated platinum(II) complexes of 2,6-diphenylpyridine bearing various π-acid donor auxiliaries. In addition, evidence of polymorphism and vapochromic behavior attributed to disruption of $\pi-\pi$ contacts by solvent molecules are described for a binuclear species. The impact of $\pi-\pi$ stacking interactions upon the spectroscopic properties of these d^8 metal complexes is highlighted.

Experimental Section

General Procedures. All starting materials were used as received from commercial sources. Solvents were of analytical grade and purified according to literature methods.[32] Elemental analyses were performed by the Institute of Chemistry at the Chinese Academy of Sciences, Beijing. Fast atom bombardment (FAB) mass spectra were obtained on a Finnigan Mat 95 mass spectrometer. ^{1}H (300 MHz), ^{13}C (126 MHz), and ^{31}P (202 MHz) NMR spectra were recorded on DPX300 and 500 Bruker FT-NMR spectrometers with chemical shifts (in ppm) relative to tetramethylsilane (for ^{1}H and ^{13}C NMR) and external H_3PO_4 (for ^{31}P NMR), respectively. Infrared spectra were recorded on a BIO RAD FT-IR spectrometer. UV−vis spectra were recorded on a Perkin-Elmer Lambda 19 UV/vis spectrophotometer. Emission spectra were obtained on a SPEX Fluorolog-2 Model F111 fluorescence spectrophotometer. Emission lifetime measurements were performed with a Quanta Ray DCR-3 pulsed Nd:YAG laser system (pulse output 355 nm, 8 ns). Errors for λ values ($\pm$ 1 nm) and τ ($\pm$ 10%) are estimated.

Synthesis. [Pt(C^N^C)dmso] (dmso = dimethyl sulfoxide) was prepared by modification of Rourke's method.[31] To a mixture of K_2PtCl_4 (0.42 g, 1.0 mmol) and 2,6-diphenylpyridine (0.23 g, 1.0 mmol) in glacial acetic acid (80 mL) was added tetrabutylammonium chloride (0.03 g, ca. 0.10 mmol). The mixture was refluxed for 8 h to give a green-yellow suspension. The Cl-bridged dimer was filtered off, washed with water and acetone, and then dissolved in boiling dmso (1 mL). The resulting yellow solution was filtered, and water (40 mL) was

(10) (a) Mizutani, M.; Kubo, I.; Jitsukawa, K.; Masuda, H.; Einaga, H. *Inorg. Chem.* **1999**, *38*, 420. (b) Hao, L.; Lachicotte, R. J.; Gysling, H. J.; Eisenberg, R. *Inorg. Chem.* **1999**, *38*, 4616. (c) Oskui, B.; Mintert, M.; Sheldrick, W. S. *Inorg. Chim. Acta* **1999**, *287*, 72. (d) Sugimori, T.; Masuda, H.; Ohata, N.; Koiwai, K.; Odani, A.; Yamauchi, O. *Inorg. Chem.* **1997**, *36*, 576, and references therein. (e) Shionoya, M.; Ikeda, T.; Kimura, E.; Shiro, M. *J. Am. Chem. Soc.* **1994**, *116*, 3848. (f) Kickham, J.; Leob, S. J.; Murphy, S. L. *J. Am. Chem. Soc.* **1993**, *115*, 7031.

(11) Braga, D.; Grepioni, F.; Desiraju, G. R. *Chem. Rev.* **1998**, *98*, 1375.

(12) Yip, H. K.; Che, C. M.; Zhou, Z. Y.; Mak, T. C. W. *J. Chem. Soc., Chem. Commun.* **1992**, 1369.

(13) Chan, C. W.; Lai, T. F.; Che, C. M.; Peng, S. M. *J. Am. Chem. Soc.* **1993**, *115*, 11245.

(14) Tse, M. C.; Cheung, K. K.; Chan, M. C. W.; Che, C. M. *Chem. Commun.* **1998**, 2295.

(15) (a) Lai, S. W.; Chan, M. C. W.; Cheung, T. C.; Peng, S. M.; Che, C. M. *Inorg. Chem.* **1999**, *38*, 4046. (b) Cheung, T. C.; Cheung, K. K.; Peng, S. M.; Che, C. M. *J. Chem. Soc., Dalton Trans.* **1996**, 1645.

(16) Lai, S. W.; Cheung, T. C.; Chan, M. C. W.; Cheung, K. K.; Peng, S. M.; Che, C. M. *Inorg. Chem.* **2000**, *39*, 255.

(17) Wong, K. H.; Cheung, K. K.; Chan, M. C. W.; Che, C. M. *Organometallics* **1998**, *17*, 3505.

(18) Lai, S. W.; Chan, M. C. W.; Cheung, K. K.; Che, C. M. *Inorg. Chem.* **1999**, *38*, 4262.

(19) Lai, S. W.; Chan, M. C. W.; Cheung, K. K.; Che, C. M. *Organometallics* **1999**, *18*, 3327.

(20) Lai, S. W.; Chan, M. C. W.; Cheung, K. K.; Peng, S. M.; Che, C. M. *Organometallics* **1999**, *18*, 3991.

(21) Scudder, M. L.; Goodwin, H. A.; Dance, I. G. *New J. Chem.* **1999**, *23*, 695.

(22) Hissler, M.; Connick, W. B.; Geiger, D. K.; McGarrah, J. E.; Lipa, D.; Lachicotte, R. J.; Eisenberg, R. *Inorg. Chem.* **2000**, *39*, 447.

(23) Büchner, R.; Cunningham, C. T.; Field, J. S.; Haines, R. J.; McMillin, D. R.; Summerton, G. C. *J. Chem. Soc., Dalton Trans.* **1999**, 711.

(24) Connick, W. B.; Marsh, R. E.; Schaefer, W. P.; Gray, H. B. *Inorg. Chem.* **1997**, *36*, 913.

(25) Bardwell, D. A.; Thompson, A. M. W. C.; Jeffery, J. C.; McCleverty, J. A.; Ward, M. D. *J. Chem. Soc., Dalton Trans.* **1996**, 873.

(26) (a) Roundhill, D. M.; Gray H. B.; Che, C. M. *Acc. Chem. Res.* **1989**, *22*, 55. (b) Miskowski, V. M.; Houlding, V. H. *Inorg. Chem.* **1989**, *28*, 1529. (c) Houlding, V. H.; Miskowski, V. M. *Coord. Chem. Rev.* **1991**, *111*, 145. (d) Cummings, S. D.; Eisenberg, R. *J. Am. Chem. Soc.* **1996**, *118*, 1949. (e) Yip, J. H. K.; Suwarno; Vittal, J. J. *Inorg. Chem.* **2000**, *39*, 3537, and references therein. (f) DePriest, J.; Zheng, G. Y.; Goswami, N.; Eichhorn, D. M.; Woods, C.; Rillema, D. P. *Inorg. Chem.* **2000**, *39*, 1955.

(27) For example, see: (a) Peyratout, C. S.; Aldridge, T. K.; Crites, D. K.; McMillin, D. R. *Inorg. Chem.* **1995**, *34*, 4484. (b) Kunugi, Y.; Mann, K. R.; Miller, L. L.; Exstrom, C. L. *J. Am. Chem. Soc.* **1998**, *120*, 589. (c) Wong, K. H.; Chan, M. C. W.; Che, C. M. *Chem. Eur. J.* **1999**, *5*, 2845. (d) Wu, L. Z.; Cheung, T. C.; Che, C. M.; Cheung, K. K.; Lam, M. H. W. *Chem. Commun.* **1998**, 1127.

(28) Miskowski, V. M.; Houlding, V. H. *Inorg. Chem.* **1991**, *30*, 4446.

(29) Charmant, J. P. H.; Forniés, J.; Gómez, J.; Lalinde, E.; Merino, R. I.; Moreno, M. T.; Orpen, A. G. *Organometallics* **1999**, *18*, 3353.

(30) (a) Maestri, M.; Deuschel-Cornioley, C.; von Zelewsky, A. *Coord. Chem. Rev.* **1991**, *111*, 117. (b) Deuschel-Cornioley, C.; Ward, T.; von Zelewsky, A. *Helv. Chim. Acta* **1988**, *71*, 130.

(31) (a) Cave, G. W. V.; Alcock, N. W.; Rourke, J. P. *Organometallics* **1999**, *18*, 1801. (b) Cave, G. W. V.; Fanizzi, F. P.; Deeth, R. J.; Errington, W.; Rourke, J. P. *Organometallics* **2000**, *19*, 1355.

(32) Perrin, D. D.; Armarego, W. L. F.; Perrin, D. R. *Purification of Laboratory Chemicals*, 2nd ed.; Pergamon: Oxford, 1980.

added to the hot filtrate. The precipitate was collected and purified by column chromatography (neutral alumina, CH_2Cl_2 as eluent) to give golden yellow crystals (0.41 g, 83%).

[Pt(C^N^C)^{t}Bupy] (1). A mixture of [Pt(C^N^C)dmso] (0.05 g, 0.10 mmol) and excess 4-*tert*-butylpyridine (25 μL, 0.17 mmol) in chloroform (10 mL) was stirred for 12 h under N_2 atmosphere at room temperature. The resulting solution was evaporated to dryness, then purified by column chromatography (neutral alumina, CH_2Cl_2 as eluent) to give golden yellow crystals (0.05 g, 96%). Anal. Calcd for $C_{26}H_{24}N_2Pt$: C, 55.81; H, 4.32; N, 5.01. Found: C, 55.80; H, 4.33; N, 4.63. FAB-MS: *m/z* 560 [M^+ + H]. ^{1}H NMR (CD_2Cl_2): 8.96 (d with ^{195}Pt satellites, 2H, ^3J = 6.8 Hz, $^3J_{PtH}$ = 43.6 Hz), 7.50 (t, 1H, ^3J = 7.8 Hz), 7.48 (d, 2H, ^3J = 7.2 Hz), 7.43 (d, 2H, ^3J = 7.8 Hz), 7.27 (d, 2H, ^3J = 7.1 Hz), 7.23 (t, 2H, ^3J = 7.8 Hz), 7.08 (t, 2H, ^3J = 7.8 Hz), 6.99 (d with ^{195}Pt satellites, 2H, ^3J = 7.8 Hz, $^4J_{PtH}$ = 24.2 Hz), 1,44 (s, 9H, CMe_3). ^{13}C{^{1}H} NMR ($CDCl_3$): 171.9, 168.1, 160.9, 153.1, 149.4, 139.3, 133.2, 130.4, 123.9, 123.6, 123.3, 114.2, 35.2 (*C*Me_3), 30.3 (C*Me*$_3$).

[Pt(C^N^C)MQ]PF$_6$ (2(PF$_6$)). A mixture of [Pt(C^N^C)-dmso] (0.05 g, 0.10 mmol) and 1-methyl-4,4′-bipyridinium (MQ^+) hexafluorophosphate (0.03 g, 0.10 mmol) in dichloromethane/acetone (5:5 mL) was stirred under N_2 atmosphere at room temperature for 48 h. The resultant suspension was evaporated to dryness. The crude solid was washed with acetone then dichloromethane and twice recrystallized from acetone/ether to give orange needles (0.06 g, 80%). Anal. Calcd for $C_{28}H_{22}N_3PtPF_6$: C, 45.41; H, 2.99; N, 5.67. Found: C, 45.37; H, 2.98; N, 5.67. FAB-MS: *m/z* 596 [M^+ + H]. ^{1}H NMR (acetone-d_6): 9.37 (d, 2H, ^3J = 6.8 Hz), 9.32 (d with ^{195}Pt satellites, 2H, ^3J = 6.8 Hz, $^3J_{PtH}$ = 44.9 Hz), 8.90 (d, 2H, ^3J = 6.8 Hz), 8.30 (d, 2H, ^3J = 6.8 Hz), 7.75 (t, 1H, ^3J = 7.6 Hz), 7.58 (d, 2H, ^3J = 6.8 Hz), 7.51 (d with ^{195}Pt satellites, ^3J = 7.6 Hz, $^4J_{PtH}$ = 10.3 Hz), 7.12 (t, 2H, ^3J = 6.9 Hz), 7.02 (t, 2H, ^3J = 7.4 Hz), 6.87 (d with ^{195}Pt satellites, 2H, ^3J = 7.0 Hz, $^3J_{PtH}$ = 24.8 Hz), 4.75 (s, 3H, Me). ^{13}C{^{1}H} NMR (DMSO-d_6): 166.0, 165.7, 151.5, 150.6, 149.1, 145.8, 142.0, 140.5, 136.0, 130.0, 124.6, 124.3, 124.2, 121.5, 115.3, 47.3 (Me).

[Pt$_2$(C^N^C)$_2$(μ-pyr)] (3). A mixture of [Pt(C^N^C)dmso] (0.05 g, 0.10 mmol) and pyrazine (4 mg, 0.05 mmol) in dichloromethane (10 mL) was stirred under N_2 atmosphere at room temperature for 48 h. The resultant deep red suspension was collected, washed with dichloromethane, and twice recrystallized from boiling chloroform to give deep red needles (0.04 g, 75%). Anal. Calcd for **3**·$CHCl_3$, $C_{39}H_{27}N_4Cl_3Pt_2$: C, 44.69; H, 2.60; N, 5.35. Found: C, 44.84; H, 2.58; N, 5.54. FAB-MS: *m/z* 929 [M^+ + H]. ^{1}H NMR (DMSO-d_6): 8.65 (s, 4H, pyrazine), 7.83 (t, 2H, ^3J = 8.1 Hz), 7.76 (d with ^{195}Pt satellites, 4H, ^3J = 7.4 Hz, $^3J_{PtH}$ = 15.4 Hz), 7.64 (m, 8H), 7.19 (t, 4H, ^3J = 7.3 Hz), 7.07 (t, 4H, ^3J = 7.4 Hz). ^{13}C{^{1}H} NMR (DMSO-d_6): 166.1, 165.8, 149.2, 145.0, 142.1, 136.1, 130.1, 124.4, 124.3. 115.4.

[Pt(C^N^C)CN(C$_6$H$_3$Me$_2$-2,6)] (4). The procedure for **1** was adopted using excess 2,6-dimethylphenylisocyanide. Yield: 0.05 g, 95%. Anal. Calcd for $C_{26}H_{20}N_2Pt$: C, 56.21; H, 3.63; N, 5.04. Found: C, 55.89; H, 3.46; N, 4.69. FAB-MS: *m/z* 556 [M^+ + H]. IR (Nujol): ν 2155 (C≡N) cm^{-1}. ^{1}H NMR ($CDCl_3$): 7.78 (d with ^{195}Pt satellites, 2H, ^3J = 7.1 Hz, $^3J_{PtH}$ = 25.6 Hz), 7.63 (t, 1H, ^3J = 8.0 Hz), 7.49 (d, 2H, ^3J = 7.6 Hz), 7.35−7.18 (m, 7H), 7.12 (t, 2H, ^3J = 7.5 Hz), 2.58 (s, 6H, Me). ^{13}C{^{1}H} NMR ($CDCl_3$): 168.0, 167.7, 149.8, 140.9, 138.6, 134.6, 131.4, 128.4, 128.1, 124.4, 124.3, 115.1, 19.2 (Me).

[Pt(C^N^C)PCy$_3$] (5). The procedure for **1** was adopted using tricyclohexylphosphine. Yield: 0.07 g, 96%. Anal. Calcd for $C_{35}H_{44}NPPt$: C, 59.65; H, 6.29; N, 1.99. Found: C, 59.31; H, 6.18; N, 1.79. FAB-MS: *m/z* 706 [M^+ + H]. ^{1}H NMR ($CDCl_3$): 7.76 (d with ^{195}Pt satellites, 2H, ^3J = 7.4 Hz, $^3J_{PtH}$ = 25.2 Hz), 7.60 (t, 1H, ^3J = 7.9 Hz), 7.46 (d, 2H, ^3J = 7.6 Hz), 7.31 (d, 2H, ^3J = 7.9 Hz), 7.15 (t, 2H, ^3J = 7.4 Hz), 7.04 (t, 2H, ^3J = 7.4 Hz), 2.66 (m, 3H), 2.14 (m, 6H), 1.76−1.67 (m, 15H), 1.21 (m, 9H). ^{13}C{^{1}H} NMR ($CDCl_3$): 166.5 (d, J_{PC} = 7.0 Hz), 166.1, 151.1, 139.5, 139.1, 129.6, 124.0, 123.2, 114.7, 33.7 (d, J_{PC} = 29.6 Hz), 30.2, 27.7 (d, J_{PC} = 10.9 Hz), 26.5. ^{31}P{^{1}H} NMR ($CDCl_3$): 23.8 ($^1J_{PtP}$ = 3803 Hz).

[Pt$_2$(C^N^C)$_2$(μ-dcpm)] (6). The procedure for **1** was adopted using 2 molar equiv of [Pt(C^N^C)dmso] and 1 equiv of bis(dicyclohexylphosphino)methane. Yield: 0.06 g, 99%. Anal. Calcd for **6**·H_2O, $C_{59}H_{70}N_2OP_2Pt_2$: C, 55.57; H, 5.53; N, 2.20. Found: C, 55.88; H, 5.46; N, 1.98. FAB-MS: *m/z* 1258 [M^+ + H]. ^{1}H NMR ($CDCl_3$): 7.69 (d with ^{195}Pt satellites, 4H, ^3J = 7.2 Hz, $^3J_{PtH}$ = 19.5 Hz), 7.61 (t, 2H, ^3J = 7.8 Hz), 7.46 (d, 4H, ^3J = 7.3 Hz), 7.31 (d, 4H, ^3J = 7.8 Hz), 7.11 (t, 4H, ^3J = 7.2 Hz), 7.06 (t, 4H, ^3J = 7.2 Hz), 3.49 (t with ^{195}Pt satellites, 2H, $^2J_{PH}$ = 11.7 Hz, $^3J_{PtH}$ = 24.8 Hz), 2.80 (m, 4H), 2.56 (br s, 4H), 2.32 (br t, 4H), 1.75−1.30 (m, 20H), 1.48 (m, 4H), 1.00 (m, 8H). ^{13}C{^{1}H} NMR ($CDCl_3$): 166.1, 166.0, 150.7, 139.6, 139.4, 129.6, 123.8, 123.4, 114.5, 37.2 (br), 31.3, 31.1, 27.6, 26.5. ^{31}P{^{1}H} NMR ($CDCl_3$): 12.0 ($^1J_{PtP}$ = 3828 Hz).

[Pt(C^N^C)PPh$_3$] (7). The procedure for **1** was adopted using excess triphenylphosphine. Yield: 0.07 g, 98%. Anal. Calcd for $C_{35}H_{26}NPPt$: C, 61.22; H, 3.82; N, 2.04. Found: C, 61.26; H, 3.74; N, 1.79. FAB-MS: *m/z* 687 [M^+ + H]. ^{1}H NMR ($CDCl_3$): 7.90 (m, 6H), 7.66 (t, 1H, ^3J = 7.9 Hz,), 7.50−7.32 (m, 13H), 6.94 (t, 2H, ^3J = 7.4 Hz), 6.70 (t with ^{195}Pt satellites, 2H, ^3J = 7.4 Hz, $^4J_{PtH}$ = 7.3 Hz), 6.27 (d with ^{195}Pt satellites, 2H, ^3J = 7.5 Hz, $^3J_{PtH}$ = 26.1 Hz). ^{13}C{^{1}H} NMR ($CDCl_3$): 166.6, 165.6 (d, J_{PC} = 7.0 Hz), 150.9, 140.3, 138.8, 135.5 (d, J_{PC} = 11.6 Hz), 132.2 (d, J_{PC} = 57.3 Hz), 130.4, 129.6, 128.1 (d, J_{PC} = 10.8 Hz), 123.8, 123.5, 114.7. ^{31}P{^{1}H} NMR ($CDCl_3$): 29.9 ($^1J_{PtP}$ = 4085 Hz).

[Pt$_2$(C^N^C)$_2$(μ-dppm)] (8). The procedure for **1** was adopted using 2 molar equiv of [Pt(C^N^C)dmso] and 1 equiv of bis(diphenylphosphino)methane. Yield: 0.06 g, 97%. Anal. Calcd for $C_{59}H_{44}N_2P_2Pt_2$: C, 57.47; H, 3.60; N, 2.27. Found: C, 57.90; H, 3.87; N, 2.16. FAB-MS: *m/z* 1234 [M^+ + H]. ^{1}H NMR ($CDCl_3$): 7.83 (m, 8H), 7.63 (t, 2H, ^3J = 7.9 Hz), 7.35−7.20 (m, 8H), 7.22−7.18 (m, 12H), 6.89 (t, 4H, ^3J = 7.4 Hz), 6.74 (t, 4H, ^3J = 7.3 Hz), 6.54 (d with ^{195}Pt satellites, 4H, ^3J = 7.4 Hz, $^3J_{PtH}$ = 25.6 Hz), 4.67 (t with ^{195}Pt satellites, 2H, $^2J_{PH}$ = 12.3 Hz, $^3J_{PtH}$ = 26.5 Hz). ^{13}C{^{1}H} NMR ($CDCl_3$): 167.1 (d, J_{PC} = 7.3 Hz), 165.8, 150.5, 139.2, 138.3, 134.3 (d, J_{PC} = 12.9 Hz), 130.7 (d, J_{PC} = 55.3 Hz), 130.0, 129.0, 127.4 (d, J_{PC} = 11.1 Hz), 123.6, 122.8, 114.3, 27.5 (PCH_2P). ^{31}P{^{1}H} NMR ($CDCl_3$): 15.7 ($^1J_{PtP}$ = 4147 Hz).

[Pt$_3$(C^N^C)$_3$(μ_3-dpmp)] (9). The procedure for **1** was adopted using 3 molar equiv of [Pt(C^N^C)dmso] and 1 equiv of bis(diphenylphosphinomethyl)phenylphosphine. Yield: 0.05 g, 93%. Anal. Calcd for $C_{83}H_{62}N_3P_3Pt_3$: C, 56.02; H, 3.51; N, 2.36. Found: C, 55.80; H, 3.61; N, 2.19. FAB-MS: *m/z* 1780 [M^+ + H]. ^{1}H NMR (CD_2Cl_2): 7.77−7.65 (m, 8H), 7.53−7.46 (m, 7H), 7.25 (d, 4H, ^3J = 7.3 Hz), 7.18 (m, 4H), 7.12 (t, 2H, ^3J = 7.4 Hz), 7.08−6.97 (m, 8H), 6.90−6.80 (m, 7H), 6.79−6.76 (m, 6H), 6.35 (br, 4H), 6.17 (br, 4H), 5.62 (t, 2H, ^3J = 7.1 Hz), 5.31 (m, 2H), 5.28 (t, 2H, ^3J = 7.7 Hz), 4.59 (m, 2H). ^{13}C{^{1}H} NMR ($CDCl_3$): 167.6 (d, J_{PC} = 8.0 Hz), 166.4, 165.9 (d, J_{PC} = 6.7 Hz), 165.7, 165.6 (d, J_{PC} = 6.3 Hz), 150.5, 150.3 (d, J_{PC} = 27.0 Hz), 141.3, 139.5, 138.4, 137.3, 136.2 (d, J_{PC} = 56.3 Hz), 134.5 (d, J_{PC} = 11.1 Hz), 133.9 (d, J_{PC} = 54.9 Hz), 132.4 (dd, $^1J_{PC}$ = 47.2 Hz, $^3J_{PC}$ = 11.2 Hz), 129.9 (d, J_{PC} = 52.3 Hz), 129.4, 129.1 (d, J_{PC} = 13.6 Hz), 127.5 (dd, $^1J_{PC}$ = 47.4 Hz, $^3J_{PC}$ = 11.0 Hz), 124.7, 123.4, 123.1, 122.8, 122.3 (d, J_{PC} = 51.0 Hz), 114.3, 113.8 (d, J_{PC} = 24.5 Hz), 22.7 (br t, PCH_2P). ^{31}P{^{1}H} NMR (CD_2Cl_2): 14.8 ($^1J_{PtP}$ = 4091 Hz), 11.7 ($^1J_{PtP}$ = 4232 Hz).

X-ray Crystallography. Crystals of **1** (benzene; evaporation), **3**·$CHCl_3$ (chloroform), **4** and **7** (diethyl ether diffusion into chloroform/benzene), and **6**·$CHCl_3$·CH_3OH·$4H_2O$ (chloroform/methanol; evaporation) were obtained. Crystals of **8** exhibited two forms with different colors; the yellow form was obtained by slow diffusion of diethyl ether into chloroform/benzene solution, while the orange form (**8**·$CHCl_3$) was grown by slow evaporation of a chloroform/methanol solution. Crystal data and details of data collection and refinement for **1**, **4**, **8**

Table 1. Crystal Data

	1	**4**	**8** (yellow form)	**8**·$CHCl_3$ (orange form)
formula	$C_{26}H_{24}N_2Pt$	$C_{26}H_{20}N_2Pt$	$C_{59}H_{44}N_2P_2Pt_2$	$C_{60}H_{45}N_2P_2Cl_3Pt_2$
fw	559.58	555.55	1233.14	1352.52
color	orange	orange	yellow	orange
cryst size	0.35 × 0.20 × 0.10	0.35 × 0.20 × 0.10	0.35 × 0.25 × 0.10	0.30 × 0.25 × 0.15
cryst syst	triclinic	orthorhombic	triclinic	triclinic
space group	$P\bar{1}$ (No. 2)	*Aba*2 (No. 41)	$P\bar{1}$ (No. 2)	$P\bar{1}$ (No. 2)
a, Å	8.302(2)	17.689(3)	17.507(2)	11.605(3)
b, Å	10.160(2)	20.489(3)	23.167(3)	12.509(2)
c, Å	13.260(2)	23.089(3)	23.837(2)	18.795(4)
α, deg	89.19(2)		106.73(2)	82.35(2)
β, deg	73.53(2)		90.31(2)	75.11(2)
γ, deg	81.05(2)		108.52(2)	71.57(2)
V, Å^3	1059.0(4)	8368(3)	8729(2)	2497.7(1)
Z	2	16	2	2
D_c, g cm^{-3}	1.755	1.764	1.407	1.798
μ, cm^{-1}	66.13	66.94	48.72	58.40
F(000)	544	4288	3588	1312
$2\theta_{max}$, deg	53.1	51.2	48.6	50
no. unique data	3962	4189	26576	8780
no. obsd data for $I > 3\sigma(I)$	3679	3213	20925	7231
no. variables	262	522	871	610
R^a	0.056	0.037	0.064	0.038
$R_w{}^b$	0.070	0.045	0.087	0.055
residual *ρ*, e Å^{-3}	+0.93, −1.54	+0.81, −1.65	+1.19, −1.52	+1.32, −1.84

[a] $R = \sum||F_o| - |F_c||/\sum|F_o|$. [b] $R_w = [\sum w(|F_o| - |F_c|)^2/\sum w|F_o|^2]^{1/2}$.

(yellow form), and **8**·$CHCl_3$ (orange form) are summarized in Table 1; full crystallographic data for **3**·$CHCl_3$, **6**·$CHCl_3$·CH_3OH·$4H_2O$, and **7** are provided in the Supporting Information. All attempts to grow single crystals of complex **9** for X-ray diffraction determination failed; crystals of **9** were always twinned or easily lost solvent and crystallinity.

For **1**, **4**, and **8** (yellow form), diffraction experiments were performed at 301 K on a MAR diffractometer with graphite-monochromated Mo Kα radiation ($\lambda = 0.71073$ Å) using a 300 mm image plate detector. The images were interpreted and intensities integrated using the program DENZO.[33] For **8**·$CHCl_3$ (orange form), intensity data were collected on a Rigaku AFC7R diffractometer with graphite-monochromated Mo Kα radiation ($\lambda = 0.71073$ Å) using $\omega-2\theta$ scans.

All structures were solved by Patterson and Fourier methods (PATTY)[34] and refined by full-matrix least-squares using the software package TeXsan[35] on a Silicon Graphics Indy computer. For **1**, a crystallographic asymmetric unit consists of one molecule. In the least-squares refinement, all 29 non-H atoms were refined anisotropically, and 24 H atoms at calculated positions with thermal parameters equal to 1.3 times that of the attached C atoms were not refined. For **4**, a crystallographic asymmetric unit consists of two independent molecules. In the least-squares refinement, all 58 non-H atoms were refined anisotropically, and 40 H atoms at calculated positions were not refined. For **8** (yellow form), a crystallographic asymmetric unit consists of three independent molecules. In the least-squares refinement, a total of 18 Pt, P, and N atoms were refined anisotropically, 177 C atoms were refined isotropically, and 132 H atoms were not refined. For **8**·$CHCl_3$ (orange form), a crystallographic asymmetric unit consists of one formula unit. The Cl atoms of the solvent were disordered and were placed at 5 positions with Cl(1) to Cl(5) having occupation numbers of 0.82, 0.51, 0.40, 0.72, and 0.55, respectively. In the least-squares refinement, all 65 non-H atoms were refined anisotropically, the atoms of the solvent were refined anisotropically, and 44 H atoms at calculated positions were not refined. The H atoms of the solvent were not included in the calculation.

Results and Discussion

All complexes synthesized in this work are derived from the convenient precursor [Pt(C^N^C)dmso], which was prepared by modification of the published procedure by Rourke and co-workers.[31] Thus tetrabutylammonium chloride was used to catalyze the monocyclometalation,[36] which was dramatically accelerated (from 3 days to 8 h) at a slight loss of overall product yield (from 96 to 83%). Ligand substitution reactions of [Pt(C^N^C)-dmso] with the appropriate N-, C-, or P-donor ligands in chloroform/dichloromethane gave the corresponding complexes in good yields (Scheme 1). For **2**, **3,** and **9**, a longer reaction time was required for complete displacement of the dmso ligand. All complexes were readily purified with column chromatography except for **2** and **3**, which were recrystallized from acetone/ether and chloroform, respectively. The molecular ion for all complexes, including **9**, dominates their respective FAB mass spectrum. All ^{1}H NMR spectra are fully resolved except for complex **9**, which displays a large number of overlapping signals in the aromatic region. The ^{31}P NMR spectra of the phosphine-ligated species **5**−**9** contain one (for mono- and binuclear) or two (for trinuclear) sharp signals with ^{195}Pt satellites. The P−Pt coupling constants (3800−4250 Hz) are comparable with

(33) *DENZO*: In *The HKL Manual*−*A description of programs DENZO, XDISPLAYF and SCALEPACK*; written by Gewirth, D. with the cooperation of the program authors Otwinowski, Z., and Minor, W.; Yale University: New Haven, CT, 1995.

(34) *PATTY*: Beurskens, P. R.; Admiraal, G.; Bosman, W. P.; Garcia-Granda, S.; Gould, R. O.; Smits, J. M. M.; Smykalla, C. *The DIRDIF program system*; Technical Report of the Crystallography Laboratory; University of Nijmegen: The Netherlands, 1992.

(35) *TeXsan*: Crystal Structure Analysis Package; Molecular Structure Corporation: The Woodlands, TX, 1985 and 1992.

(36) Kvam, P.-I.; Songstad, J. *Acta Chem. Scand.* **1995**, *49*, 313.

(37) Green, M.; Howard, J. A. K.; Murray, M.; Spencer, J. L.; Stone, F. G. A. *J. Chem. Soc., Dalton Trans.* **1977**, 1509.

(38) Jovanović, B.; Manojlović-Muir, Lj.; Muir, K. W. *J. Chem. Soc., Dalton Trans.* **1972**, 1178.

(39) Lai, S. W.; Cheung, K. K.; Chan, M. C. W.; Che, C. M. *Angew. Chem., Int. Ed.* **1998**, *37*, 182.

(40) Breault, G. A.; Hunter, C. A.; Mayers, P. C. *J. Am. Chem. Soc.* **1998**, *120*, 3402.

Scheme 1

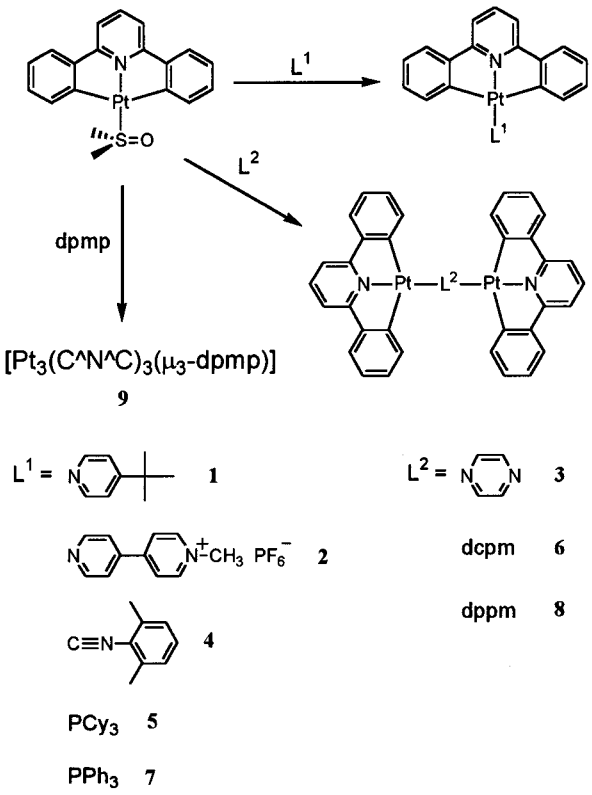

those in $[Pt(C^N^N)PPh_3]ClO_4$ and $[Pt_2(C^N^N)_2(\mu\text{-dppm})](ClO_4)_2$ (HC^N^N = 6-phenyl-2,2′-bipyridine) ($^1J_{P-Pt}$ = 4166 Hz).[15]

Crystal Structures and $\pi-\pi$ Interactions. The X-ray crystal structures of **1**, **3**·$CHCl_3$, **4**, **6**·$CHCl_3$·CH_3OH·$4H_2O$, **7**, **8** (yellow form), and **8**·$CHCl_3$ (orange form) have been determined. The [Pt(C^N^C)] motif in all structures is essentially planar, with bond parameters similar to those found in [Pt(C^N^C)dmso] and [Pt(C^N^C)CO],[31] but close Pt−Pt contacts (less than 4 Å) are not observed in the crystal lattices. Nonetheless, both intermolecular and intramolecular $\pi-\pi$ stacking interactions exist for many of the structures, and we shall describe these in detail since such interactions are expected to affect the solid-state luminescent properties of these complexes.

Figure 1*a* shows a perspective view of complex **1**. The aromatic ring of the 4-*tert*-butylpyridine ligand is nearly orthogonal to the Pt(C^N^C) plane with a dihedral angle of 106.1°; this value is comparable to the related angle of 118.3° in the structure of $[Pt(C^N^N)py]ClO_4$.[26e] As shown in Figure 1*b*, the Pt(C^N^C) units in **1** are stacked in pairs in a head-to-tail style with an interplanar separation of 3.40 Å, which is sufficiently close for weak $\pi-\pi$ interactions[3] that lead to solid-state excimeric emission (see later).

The crystal structure of complex **3** (see Supporting Information) shows two Pt(C^N^C) moieties linked by a pyrazine bridge; no $\pi-\pi$ stacking is observed in the crystal lattice. The dihedral angles between the pyrazine ring and the two Pt(C^N^C) planes (124.0° and 130.5°) deviate significantly from orthogonality, hence a degree of overlap between the 5d(Pt) and the pπ* orbitals of pyrazine is possible. We note that (a) this complex is deep red in color, which is unique with regards to this work, and (b) the proposed MLCT (5d)Pt → π*(pyrazine) transition appears at λ_{max} 456 nm in dichloromethane, which is lower in energy than the (5d)Pt → π*(C^N^C) transitions (ca. 420 nm) for other derivatives.

The perspective view of one of the two independent molecules in the crystal structure of complex **4** is shown in Figure 2*a*. The Pt−C(isocyanide) distance of 1.85(1) Å is comparable to those in $[Pt_3(^tBuNC)_6]$ (1.88(2)−1.92(2) Å)[37] and *cis*-$[PtCl_2(PhNC)_2]$ (1.90(2) Å),[38] but slightly shorter than the Pt−C(carbene) distances in $[Pt(C^N^N)(diaminocarbene)]ClO_4$ (1.989(6)−1.997(7) Å)[19] and $[Pt(CN)(C_{10}H_{21}N_4)]_6$ (1.97(1)−2.01(1) Å).[39] The dihedral

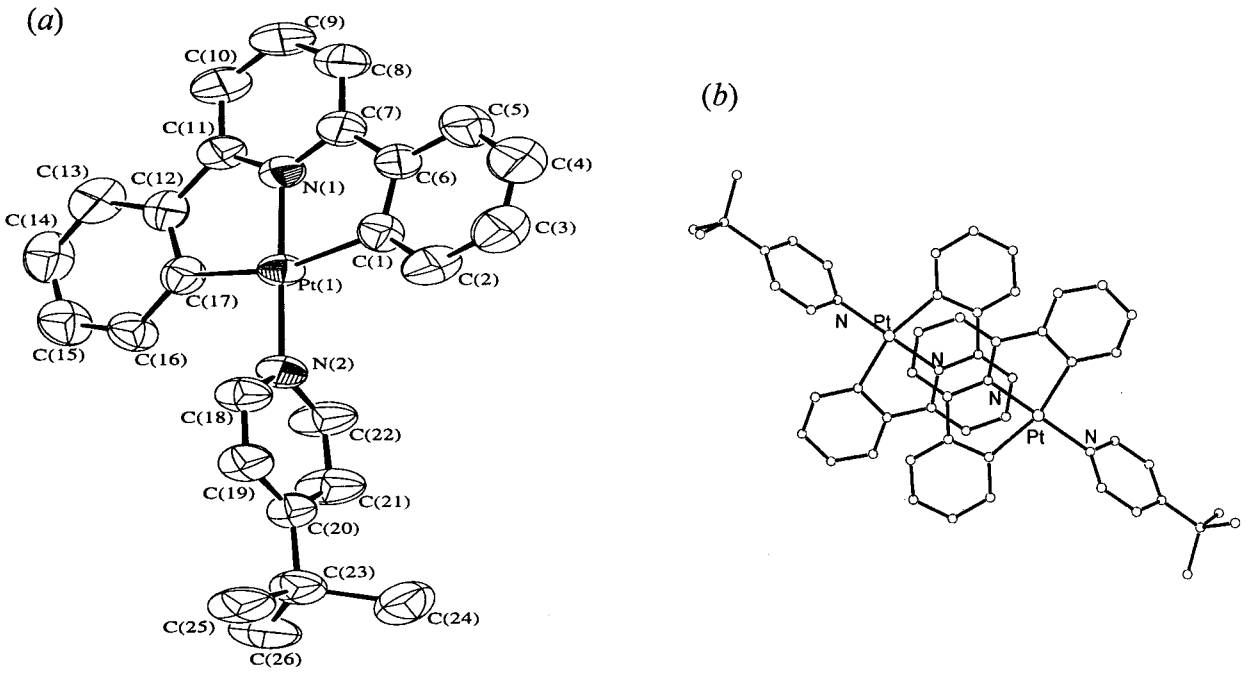

Figure 1. (*a*) Perspective view of **1** (50% probability ellipsoids). Selected bond lengths (Å) and angles (deg): Pt(1)−N(1), 1.976(8); Pt(1)−N(2), 2.042(8); N(1)−Pt(1)−N(2), 178.9(2); C(1)−Pt(1)−C(17), 161.6(4). (*b*) Crystal-packing diagram showing dimeric $\pi-\pi$ interaction.

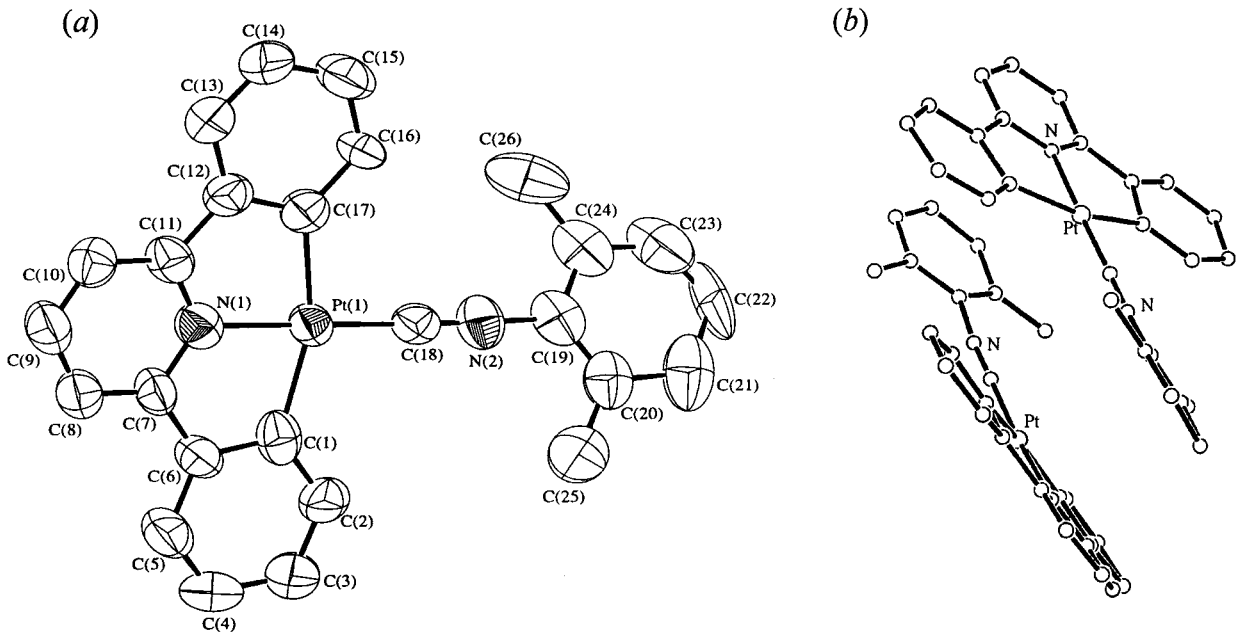

Figure 2. (*a*) Perspective view of one of the independent molecules in **4** (50% probability ellipsoids). Selected bond lengths (Å) and angles (deg): Pt(1)−N(1), 2.00(1); Pt(1)−C(18), 1.85(1); N(2)−C(18), 1.17(2); N(1)−Pt(1)−C(18), 178.9(5); C(1)−Pt(1)−C(17), 160.8(6); Pt(1)−C(18)−N(2), 178(1). (*b*) Crystal-packing diagram showing dimeric $\pi-\pi$ interaction.

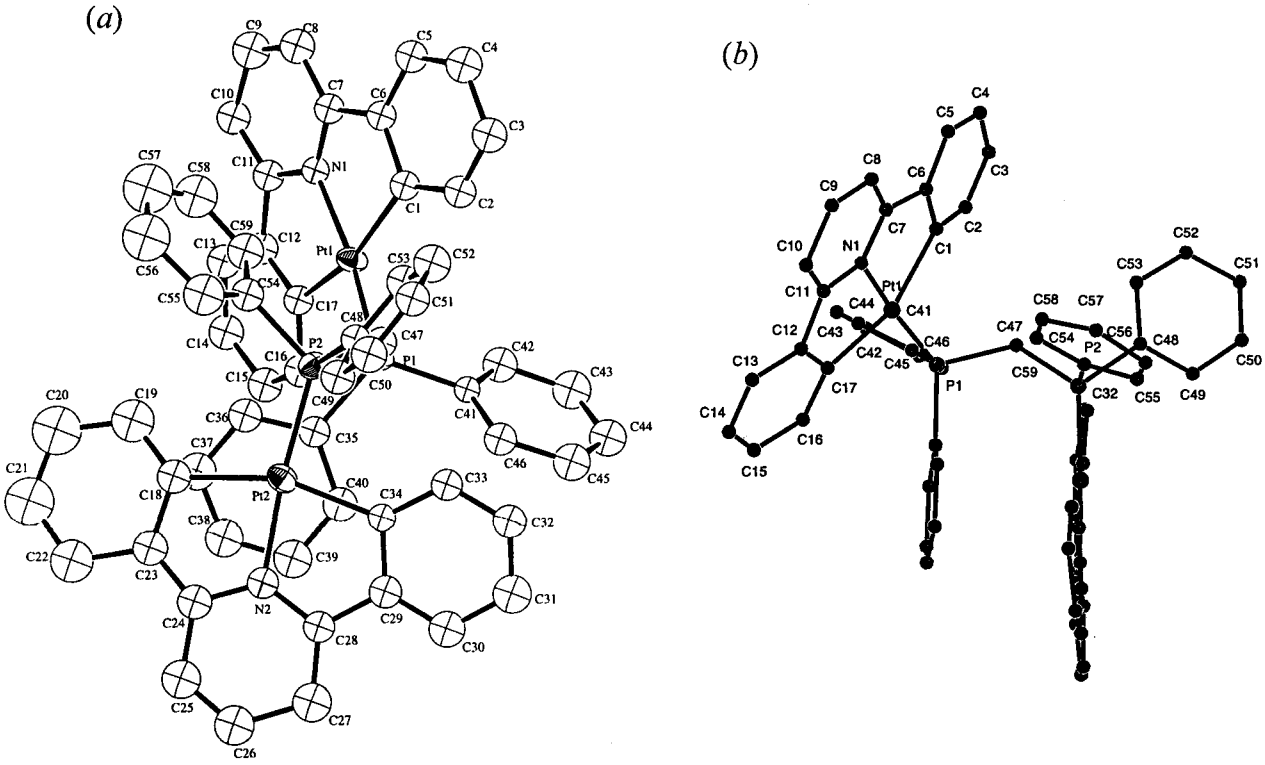

Figure 3. (*a*) Perspective view of one of the independent molecules in **8** (yellow form) (40% probability ellipsoids). Selected bond lengths (Å) and angles (deg): Pt(1)−P(1), 2.226(3); Pt(1)−N(1), 2.006(8); Pt(2)−P(2), 2.218(3); Pt(2)−N(2), 2.036(9); P(1)−Pt(1)−N(1), 171.2(2); Pt(1)−P(1)−C(47), 112.3(3); P(2)−Pt(2)−N(2), 174.6(3); Pt(2)−P(2)−C(47), 114.1(4). (*b*) Side view showing $\pi-\pi$ interaction between Pt(C^N^C) unit and phenyl ring of dppm.

angle between the ring of the 2,6-dimethylphenylisocyanide ligand and the Pt(C^N^C) plane is 28.0° and 29.1° for the two independent molecules. The crystal lattice reveals dimers interacting in a head-to-tail fashion (Figure 2*b*). Intermolecular $\pi-\pi$ stacking between the phenyl ring and the Pt(C^N^C) fragment is separated by 3.39 Å.

For complex **7** (see Supporting Information), the P−Pt distance is 2.2156(9) Å, which is similar to that in [Pt(C^N^N)PPh$_3$]ClO$_4$ (2.243(3) Å).[15b] While the latter has weak $\pi-\pi$ contacts in its crystal lattice, such stacking interactions are absent in **7**, and this can explain the difference in the emissive behavior of **7** compared to the other complexes (see later).

The salient structural result in this work is the crystallographic elucidation of two forms of the same

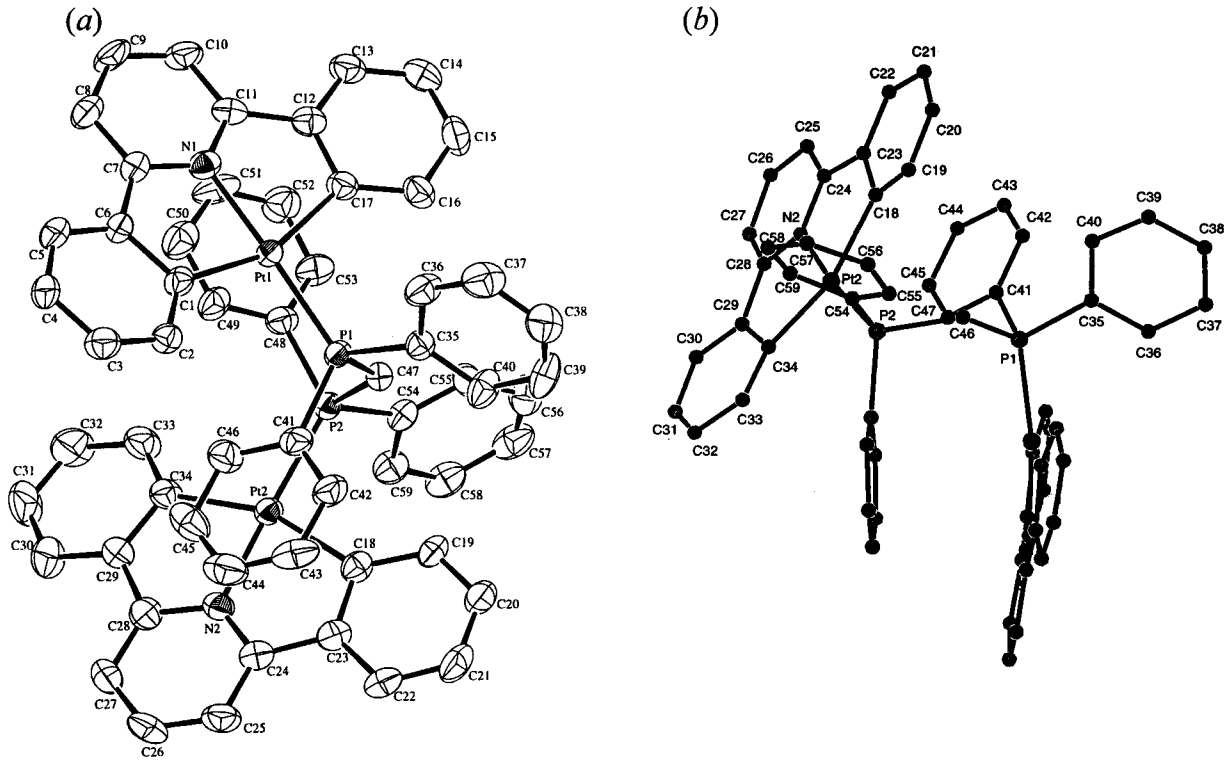

Figure 4. (*a*) Perspective view of the complex molecule in **8**·$CHCl_3$ (orange form) (50% probability ellipsoids). Selected bond lengths (Å) and angles (deg): Pt(1)−P(1), 2.220(2); Pt(1)−N(1), 2.024(6); Pt(2)−P(2), 2.214(2); Pt(2)−N(2), 2.012(6); P(1)−Pt(1)−N(1), 170.6(2); Pt(1)−P(1)−C(47), 114.1(2); P(2)−Pt(2)−N(2), 172.4(2); Pt(2)−P(2)−C(47), 114.4(2). (*b*) Side view showing two $\pi-\pi$ interactions between Pt(C^N^C) units and phenyl rings of dppm.

Table 2. UV−Vis Absorption Data (in CH_2Cl_2 at 298 K unless otherwise stated)

complex	λ_{max}/nm (ϵ/dm^3 mol^{-1} cm^{-1})
[Pt(C^N^C)^{t}Bupy] (**1**)	255 (32750); 269 (33060); 281 (36410); 309 (12150); 337 (sh, 10130); 348 (11290); 440 (sh, 430); 512 (90)
[Pt(C^N^C)MQ] PF_6 (**2**(PF_6))	252 (50310); 276 (47850); 305 (sh, 13240); 339 (sh, 12160); 352 (13360); 410 (sh, 9120); 510 (sh,1540)[a]
[Pt_2(C^N^C)$_2$(μ−pyr)] (**3**)	252 (78620); 278 (73210); 339 (22030); 350 (22190); 456 (17280); 510 (sh, 8320)
[Pt(C^N^C)CN($C_6H_3Me_2$-2,6)] (**4**)	245 (32460); 285 (23120); 337 (12060); 350 (14870); 410 (sh, 420); 440 (sh, 290); 514 (40)
[Pt(C^N^C)PCy_3] (**5**)	250 (31000); 277 (26130); 330 (sh, 8210); 348 (11200); 430 (sh, 420); 510 (sh, 40)
[Pt_2(C^N^C)$_2$(μ-dcpm)] (**6**)	248 (56710); 280 (51350); 335 (sh, 18380); 351 (21520); 430 (sh, 1210); 510 (sh, 160)
[Pt(C^N^C)PPh_3] (**7**)	250 (30340); 283 (24700); 335 (sh, 9280); 350 (14040); 412 (450); 435 (sh, 390); 509 (50)
[Pt_2(C^N^C)$_2$(μ-dppm)] (**8**)	250 (58900); 280 (45620); 335 (sh, 16960); 350 (18920); 430 (sh, 1520); 490 (sh, 320); 510 (sh, 210)
[Pt_3(C^N^C)$_3$(μ_3-dpmp)] (**9**)	246 (81360); 280 (sh, 67330); 340 (sh, 28120); 351 (31590); 430 (sh, 4850);490 (sh, 1520); 510 (sh, 970)

[a] Measured in acetonitrile.

complex, namely, the yellow and orange forms of **8**, which reveal the absence and presence of solvent molecules ($CHCl_3$) in the respective crystal lattice. A perspective view of one of the three independent molecules in **8** (yellow form) is shown in Figure 3*a*. The P−Pt distances are similar to those in **7**. The three independent molecules in the asymmetric unit are virtually identical, and all exhibit the following feature: one of the Pt(C^N^C) planes engages in weak intramolecular $\pi-\pi$ stacking with an adjacent phenyl ring of the dppm ligand (Figure 3*b*), and interplanar separations ranging from 3.38 to 3.67 Å are evident. Figure 4*a* depicts the perspective view of the complex molecule in **8**·$CHCl_3$ (orange form). Two $\pi-\pi$ interactions are found between each Pt(C^N^C) unit and a phenyl ring from different phosphorus atoms of the dppm ligand (Figure 4*b*). The $\pi-\pi$ interplanar distances of 3.12 and 3.29 Å are noticeably shorter than in the yellow form of **8**. We thus infer that different intramolecular $\pi-\pi$ interactions are responsible for the yellow and orange crystalline forms of complex **8**. For **8**·$CHCl_3$, it is somewhat surprising that the inclusion of a solvent molecule alters the crystal packing such that an additional intramolecular $\pi-\pi$ interaction is afforded. This phenomenon is further investigated by studying the vapochromic behavior of **8** (see later). The influence of solvent on aromatic interactions in metal tris-bipyridine complexes has been studied by Hunter and co-workers using ^{1}H NMR chemical shifts and NOE experiments.[40] The contrast between these intramolecular π-stacking

Table 3. Emission Data (λ_{ex} = 350−355 nm)

complex	alcoholic glass[a] λ_{max}/nm (τ/μs)	solid, 298 K λ_{max}/nm (τ/μs)	solid, 77 K λ_{max}/nm (τ/μs)
[Pt(C^N^C)^{t}Bupy] (**1**)	484, 520 (16); 622 (2.2)	611 (0.17)	642 (1.3)
[Pt(C^N^C)MQ] PF_6 (**2**(PF_6))	480, 517 (14)	686 (≤0.1)	709 (0.2)
[Pt_2(C^N^C)$_2$(μ-pyr)] (**3**)	481, 508 (24), 545 (sh)	658 (0.21)	689 (2.0)
[Pt(C^N^C)CN($C_6H_3Me_2$-2,6)] (**4**)	518 (8.4); 598 (6.0)	566 (0.61)	590 (4.4)
[Pt(C^N^C)PCy_3] (**5**)	522 (36); 636 (5.6)	618 (≤0.1)	640 (1.8)
[Pt_2(C^N^C)$_2$(μ-dcpm)] (**6**)	524 (15); 601 (6.2)	623 (≤0.1)	621 (1.1)
[Pt(C^N^C)PPh_3] (**7**)	512 (13), 551	568 (0.74)	588 (5.6)
[Pt_2(C^N^C)$_2$(μ-dppm)] (**8**)	525 (13); 604 (9.1)	624 (0.25)	633 (4.4)
[Pt_3(C^N^C)$_3$(μ_3-dpmp)] (**9**)	526 (11); 596 (8.2)	633 (1.4)	648 (4.3)

[a] Measured in methanol/ethanol = 1:5 (v/v) at 77 K, complex concentration ~5 × 10^{-5} M.

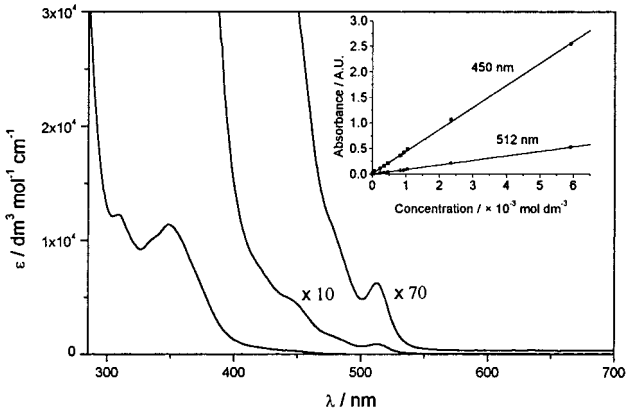

Figure 5. UV−vis absorption spectrum of **1** in dichloromethane at 298 K (inset: plots of absorbance at 450 (R = 0.99) and 512 (R = 0.99) nm versus concentration).

interactions and those in the related binuclear complexes [M_2(C^N^N)$_2$(μ-dppm)](ClO_4)$_2$ (M = Pt,[15a] Pd[16]) and [Au_2(C^N^C)$_2$(μ-L)](ClO_4)$_2$ (L = dppm, dppe),[17] where cyclometalated d^8 metal units are oriented in a face-to-face manner, is striking.

The crystal structure of **6** has also been elucidated (see Supporting Information); hence a comparison can be drawn between binuclear species with phenyl- and cyclohexyl-substituted bis(phosphine) bridges. Close examination of the crystal lattice revealed no intra- or intermolecular π-stacking interactions. Face-to-face approach of Pt(C^N^C) units is presumably not favorable due to coulombic repulsive interactions.

Absorption Data. The UV−vis absorption data of complexes **1**−**9** are summarized in Table 2. As a representative example, the UV−vis spectrum of **1** is shown in Figure 5. Comparisons with the absorption data of the Au(III) analogues[17] are pertinent for assignment purposes. There are characteristic vibronically structured absorptions for all complexes at 335−353 nm (ϵ > 10^4 dm^3 mol^{-1} cm^{-1}). The vibronic progressions (ca. 1300 cm^{-1}) are in close agreement with the skeletal vibrational frequency of the C^N^C ligand and are independent of the auxiliary ligands. These diagnostic absorptions, which appear at higher energies than for the Au(III) counterparts (380−405 nm), are assigned to a metal-perturbed intraligand transition. Likewise, blue-shifted intraligand transitions from gold to platinum have been observed for the [M(^{t}Bu_3tpy)Cl]$^{n+}$ (M = Pt, n = 1; M = Au, n = 2; ^{t}Bu_3tpy = 4,4′,4″-tri-*tert*-butyl-2,2′:6′,2″-terpyridine)[18] and [M(*p*-MeOPhC^N^N)Cl]$^{n+}$ (M = Pt, n = 0;[15a] M = Au, n = 1;[41] *p*-MeOPh(HC^N^N) = 4-(*p*-methoxyphenyl)-6-phenyl-2,2′-bipyridine) complexes.

Except for **2** and **3**, all complexes show a modest shoulder at ca. 440 nm ($\epsilon \approx$ 500 dm^3 mol^{-1} cm^{-1}) and a weak band at 509−515 nm (ϵ < 10^2 dm^3 mol^{-1} cm^{-1}). These absorptions are absent in the UV−vis spectra of the Au(III) analogues[17] but are similar in energy to the proposed MLCT transitions of the related Pt(II) terpyridine[18,42] and cyclometalated diimine[15,19,26e] derivatives. Complex **1** was chosen as an illustrative example to study the effects of varying solvents and complex concentration upon absorption spectra. The absorption spectrum of **1** in dichloromethane obeys Beer's law at concentrations ranging from 1 × 10^{-5} to 6 × 10^{-3} mol dm^{-3}, as evidenced by the linear plots of the absorbance at 450 and 512 nm versus concentration (Figure 5: inset), hence no ground state oligomerization processes is implied. The 512 nm absorption does not exhibit remarkable solvatochromic effects (see Supporting Information) and a ligand-field transition is unlikely to occur in this spectral region in view of the strong σ-donor strength of the trans-cyclometalating ligand. A spin-forbidden transition with admixture of both ^{3}MLCT [(5d)Pt → π*(C^N^C)] and ^{3}IL [π → π*] characters is therefore proposed for the 512 nm band, while the shoulder at 420−460 nm is assigned as ^{1}MLCT (5d)Pt → π*(C^N^C) in nature. Connick et al.[43] concluded that the ^{3}IL and ^{3}MLCT transitions are heavily mixed in Pt(II) diimine complexes, and we extend this notion to the lowest energy transition in the [Pt(C^N^C)] system.

For complexes **2** and **3**, there is an absorption at λ_{max} 410 and 456 nm, respectively, in addition to the vibronic ^{1}IL band at λ_{max} 350 nm (see Supporting Information). Both the 1-methyl-4,4′-bipyridinium ion and pyrazine are expected to have lower π* energies than the C^N^C ligand, and we therefore tentatively assign these absorptions to the respective ^{1}MLCT (L = MQ^+, pyr) transitions.

Emission Data. All complexes are photoluminescent in the solid state and in 77 K methanol/ethanol (1:5, v/v) glass, but no emission is detected in dichloromethane at room temperature. The emission data of **1**−**9** are summarized in Table 3.

As with the absorption spectra, the auxiliary ligand L in [Pt(C^N^C)L] has minimal effect on the emission maxima. The dilute (~5 × 10^{-5} mol dm^{-3}) 77 K alcoholic glasses of **1**−**9** exhibit structured emissions (λ_{max} of most intense band = 508−526 nm) with vibronic spacings in the 1200−1300 cm^{-1} range, which matches the skeletal vibrational frequency of (C^N^C) (Figure 6 for **7**, **8**, and

(41) Liu, H. Q.; Cheung, T. C.; Peng, S. M.; Che, C. M. *J. Chem. Soc., Chem. Commun.* **1995**, 1787.
(42) Bailey, J. A.; Hill, M. G.; Marsh, R. E.; Miskowski, V. M.; Schaefer, W. P.; Gray, H. B. *Inorg. Chem.* **1995**, *34*, 4591.
(43) Connick, W. B.; Miskowski, V. M.; Houlding, V. H.; Gray, H. B. *Inorg. Chem.* **2000**, *39*, 2585.

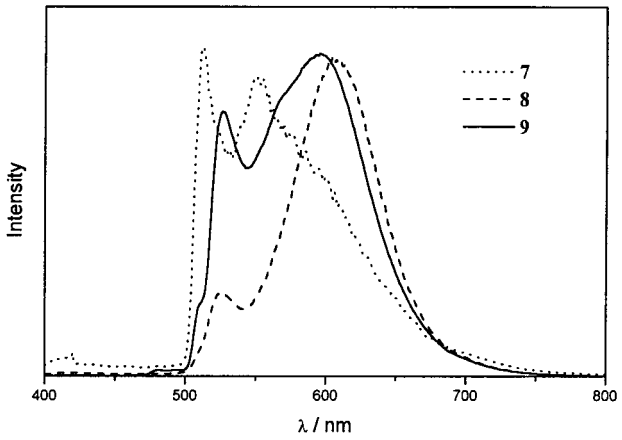

Figure 6. Emission spectra of **7**, **8**, and **9** in methanol/ethanol (1:5, v/v) glass at 77 K (5×10^{-5} M, $\lambda_{ex} = 350$ nm, normalized intensities).

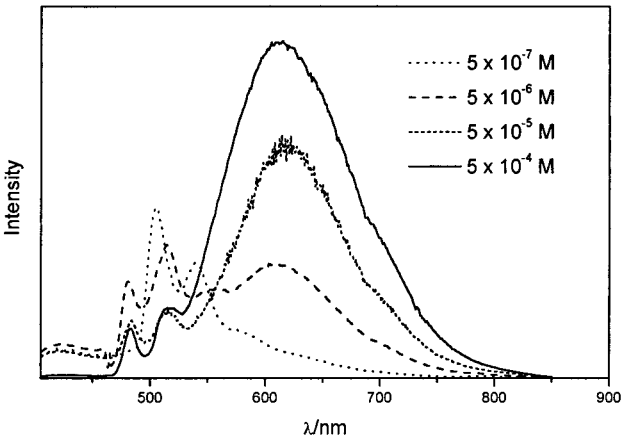

Figure 7. Emission spectra of **1** at different concentrations in methanol/ethanol/DMF (5:5:1) glass at 77 K ($\lambda_{ex} = 350$ nm).

9). These emission bands are accredited to metal-perturbed $^3\pi\pi^*$ states, like for related $[Pt(^tBu_3tpy)Cl]^+$,[18] $[Pd(C^N^N)L]^+$,[16] and $[Au(C^N^C)L]^+$,[17] complexes. Significantly, broad unstructured emission bands at lower energies (λ_{max} 596−636 nm) are also observed for **1**, **4**−**6**, **8**, and **9**. The structural data for **1**, **4**, **8**, and **8**·$CHCl_3$ show that π-stacking of aromatic moieties exist in the crystal lattice. According to Gray and co-workers for $[Pt(tpy)Cl]ClO_4$ (tpy = 2,2′:6′,2″-terpyridine)[42] and as reported by our group for $[Pt(C^N^N)PPh_3]ClO_4$,[15b] such $\pi-\pi$ contacts can give rise to excimeric emissions that are red-shifted in energy from the corresponding ^{3}IL emissions. Similarly, the formation of $^3\pi\pi^*$ excimers in 77 K glasses upon light excitation may account for the low-energy emissions from these [Pt(C^N^C)] complexes.

The emission spectra of complexes **1** and **4**−**9** in 77 K methanol/ethanol/DMF (5:5:1) glasses at various complex concentrations have also been examined to further probe the low-energy luminescence. The results obtained for **1** are shown in Figure 7. Upon increasing the complex concentration from 5×10^{-7} to 5×10^{-4} mol dm^{-3}, a broad unstructured peak at λ_{max} 622 nm develops at the expense of the high-energy vibronic emission at λ_{max} 520 nm. Similar behavior has also been observed for **4**−**6**, but not for **7**−**9**, which have arylphosphine auxiliary ligands. In the case of **7**, no unstructured low-energy emission was recorded even at a complex concentration of 1×10^{-3} mol dm^{-3}. This indicates that there is no $\pi-\pi$ interaction between the excited and ground states of complex **7**. In contrast, for **8** and **9**, the low-energy band around 600 nm remains dominant at concentrations as low as 5×10^{-7} mol dm^{-3}. It is judicious to note that intermolecular $\pi-\pi$ interactions are unlikely to occur at such a low concentration and *intramolecular* $\pi-\pi$ interactions between Pt(C^N^C) moieties and phenyl rings are apparent in the crystal lattices of **8** and **8**·$CHCl_3$. These types of contacts may be envisaged to yield excimeric emissions for **8** and **9** even in diluted glassy solutions. In contrast, for **1** and **4**−**6**, we suggest that *intermolecular* $\pi-\pi$ interactions between aromatic substituents give rise to the excimeric emissions, and these interactions are affected by complex concentration in the alcoholic glasses.

The luminescence of **9** in diluted methanol/ethanol (1:5, v/v) glass experiences a color change from bright orange to weak red and finally diminishes as the temperature is gradually increased from 77 to 298 K. Although the reason for this phenomenon has not been elucidated, we suggest that this photophysical change in emissive properties is related to the perturbation of weak inter- and intramolecular $\pi-\pi$ interactions.

The 298 K solid-state emission spectra of **1**, **4**−**6**, **8**, and **9** are characterized by a broad, unstructured band at λ_{max} 566−633 nm, which red-shifts in energy upon cooling to 77 K. These emissions are comparable in energy to those in 77 K alcoholic glasses (see Supporting Information for **4**) and are similarly assigned as $^3\pi\pi^*$ excimeric in nature. The crystal lattices of **1**, **4**, **6**, and **8** revealed no close Pt−Pt contacts; hence $^3[d\sigma^* \rightarrow \pi^*]$ excited states are not invoked. A correlation is therefore proposed between low-energy excimeric emissions and $\pi-\pi$ interactions in the crystal lattices of this class of complexes.

The solid-state emission band at 298 K for complexes **2** and **3** (see Supporting Information) is observed at λ_{max} 686 and 658 nm, respectively, and they slightly red-shift at 77 K; a ^{3}MLCT (L = MQ^+ and pyr, respectively) excited state is tentatively assigned. A $^3\pi\pi^*$ excimeric excited state is not proposed because no π-stacking interactions are observed in the crystal lattice of **3**·$CHCl_3$. These low-energy emissions reflect the low π^* energy of the corresponding acceptor group.

Vapochromic Behavior of Complex 8. When an orange crystalline sample of **8** was exposed to a saturated atmosphere of dichloromethane, acetone, pentane, benzene, or methanol vapor, an immediate transformation into the bright yellow form occurred, while exposure to reduced pressure for several minutes resulted in the restoration of the original orange color. This reversible process was repeated for more than five times without any apparent change to the complex. We infer that the vapochromism displayed by **8** is due to the perturbation of $\pi-\pi$ interactions by VOCs and that the orange and yellow forms correspond to the crystal structures obtained for **8** and **8**·$CHCl_3$, respectively, which exhibit different intramolecular $\pi-\pi$ interactions in their crystal lattices. Previously, diimine Pt(II) salts have been reported to exhibit Pt−Pt polymorphism,[26,43,44] but examples such as **8**/**8**·$CHCl_3$, which involve modification of $\pi-\pi$ interactions, are scarce. However, the emission maxima and lifetimes of the orange and yellow forms

of **8** are very similar, and hence its employment as a luminescent vapochromic sensor is ineffective. Recently, van Koten and co-workers reported a reversible crystalline-state reaction of gaseous SO_2 with a nonporous crystalline material consisting of "pincer" organoplatinum(II) molecules.[45] We conceive that the vapochromic effect observed in this study can be amplified by incorporating the $[Pt_2(C^N^C)_2(\mu\text{-dppm})]$ moiety into polymers or dendrimers,[46] and this may provide access to new types of sensory materials for VOCs.[47]

Concluding Remarks

The elucidation of a number of crystal structures in this report has revealed a rich variety of π-stacking interactions for this system. The trans-cyclometalated platinum motif [Pt(C^N^C)] has been shown to form inter- and intramolecular π adducts with phenyl rings in close proximity in a face-to-face fashion, while $\pi-\pi$ attractions are also manifested for dimeric [Pt(C^N^C)] fragments in a head-to-tail manner. The observation of different overlapping π-aromatic moieties for this family of complexes is noteworthy when compared to the related [Pd(C^N^N)], [Pt(C^N^N)], and [Au(C^N^C)] systems, where π-stacking between pairs of aromatic tridentate ligands (with metal−metal interactions for Pt) are typically recognized. These types of noncovalent interactions fundamentally affect the emissive behavior of these [Pt(C^N^C)] solids.

The lowest-energy UV−vis absorption bands of Pt(C^N^C) complexes bearing 4-*tert*-butylpyridine, 2,6-dimethylphenylisocyanide, and various phosphine ligands are proposed to be an admixture of triplet (5d)Pt $\rightarrow \pi^*$(C^N^C) and $\pi \rightarrow \pi^*$ transitions. A correlation between the crystal structures and spectroscopic properties of these derivatives, and especially between solid-state $\pi-\pi$ interactions and low-energy $\pi\pi^*$ excimeric emissions, is implied by the observations herein.

Coordination of a good π-acceptor ligand to the [Pt(C^N^C)] moiety has an impact upon the low-energy MLCT transition. The ^{3}MLCT (5d)Pt $\rightarrow \pi^*$(1-methyl-4,4′-bipyridinium/pyrazine) emissions of complexes **2** and **3** occur in the red region (λ_{max} 650−700 nm) and are substantially red-shifted from other derivatives. The "saturated" red phosphorescence of $[Pt_2(C^N^C)_2(\mu\text{-pyr})]$ (**3**) may have potential applications in high-efficiency organic light-emitting devices.[48]

The use of luminescent late transition metal species for sensing applications based on perturbations of weak metal−metal contacts has been previously demonstrated.[27,32] Indeed, weak noncovalent interactions of this kind are ideal as probing components because they should be highly sensitive to environmental changes, especially if the origin and nature of the signaling element is coupled to such weak interactions (e.g., luminescence from an excited state involving metal−metal interaction). Employment of $\pi-\pi$ attractions as the monitoring device in molecular sensors is a new research direction. While the vapochromic observations in this study cannot be exploited, we are presently pursuing luminescent systems with efficient sensing capabilities based on weak $\pi-\pi$ interactions.

Acknowledgment. We are grateful for support from The University of Hong Kong and the Research Grants Council of the Hong Kong SAR, China [HKU 7298/99P].

Supporting Information Available: Tables of crystal data, atomic coordinates, calculated coordinates, anisotropic displacement parameters, and bond lengths and angles for **1**, **3**·$CHCl_3$, **4**, **6**·$CHCl_3$·CH_3OH·$4H_2O$, **7**, **8**, and **8**·$CHCl_3$; ORTEP plots of complexes of **3**, **6**, and **7**; UV−vis absorption spectra of **2** (in CH_3CN) and **3** (in CH_2Cl_2) at 298 K; emission spectra of **4** in methanol/ethanol (1:5, v/v) glass at 77 K (5×10^{-5} M) and in the solid state at 298 and 77 K; solid-state emission spectra of **2** and **3** at 298 K; listing of UV−vis absorption data for **1** in different solvents. This material is available free of charge via the Internet at http://pubs.acs.org.

OM0009839

(44) (a) Bielli, E.; Gidney, P. M.; Gillard, R. D.; Heaton, B. T. *J. Chem. Soc., Dalton Trans.* **1974**, 2133. (b) Kiernan, P. M.; Ludi, A. *J. Chem. Soc., Dalton Trans.* **1978**, 1127. (c) Daws, C. A.; Exstrom, C. L.; Sowa, J. R.; Mann, K. R. *Chem. Mater.* **1997**, *9*, 363, and references therein.

(45) Albrecht, M.; Lutz, M.; Spek, A. L.; van Koten, G. *Nature* **2000**, *406*, 970.

(46) Albrecht, M.; Gossage, R. A.; Lutz, M.; Spek, A. L.; van Koten, G. *Chem. Eur. J.* **2000**, *6*, 1431.

(47) (a) Vickery, J. C.; Olmstead, M. M.; Fung, E. Y.; Balch, A. L. *Angew. Chem., Int. Ed. Engl.* **1997**, *36*, 1179. (b) Mansour, M. A.; Connick, W. B.; Lachicotte, R. J.; Gysling, H. J.; Eisenberg, R. *J. Am. Chem. Soc.* **1998**, *120*, 1329. (c) Cariati, E.; Bourassa, J.; Ford, P. C. *Chem. Commun.* **1998**, 1623. (d) Buss, C. E.; Anderson, C. E.; Pomije, M. K.; Lutz, C. M.; Britton, D.; Mann, K. R. *J. Am. Chem. Soc.* **1998**, *120*, 7783. (e) Beauvais, L. G.; Shores, M. P.; Long, J. P. *J. Am. Chem. Soc.* **2000**, *122*, 2763. (f) Benkstein, K. D.; Hupp, J. T.; Stern, C. L. *Angew. Chem., Int. Ed.* **2000**, *39*, 2891.

(48) Baldo, M. A.; O'Brien, D. F.; You, Y.; Shoustikov, A.; Sibley, S.; Thompson, M. E.; Forrest, S. R. *Nature* **1998**, *395*, 151.